

RESPONSES OF PRIMARY PRODUCTION AND TOTAL CARBON STORAGE TO CHANGES IN CLIMATE AND ATMOSPHERIC CO₂ CONCENTRATION

X. Xiao^{1,2}, D.W. Kicklighter¹, J.M. Melillo¹,
A.D. McGuire¹, P.H. Stone² and A.P. Sokolov²

¹The Ecosystems Center, Marine Biological Laboratory, Woods Hole, MA 02543

²The Joint Program on the Science and Policy of Global Change, MIT, Cambridge, MA 02139

ABSTRACT

We used the Terrestrial Ecosystem Model (TEM, version 4.0) to estimate global responses of annual net primary production (NPP) and total carbon storage to changes in climate and CO₂ level, driven by the climate outputs from the 2-dimensional MIT L-O climate model and the 3-dimensional GISS and GFDL-q atmospheric general circulation models. For contemporary climate with 315 ppmv CO₂, TEM estimated that global NPP is 47.9 PgC/yr and global total carbon storage is 1659 PgC, including 909 PgC of vegetation carbon and 750 PgC of reactive soil organic carbon. For climate change with 522 ppmv CO₂ (corresponding to a climate change due to an effective CO₂ doubling), the responses of global NPP are +17.8% (8.6 PgC/yr) for the MIT L-O climate, +18.5% (8.9 PgC/yr) for the GFDL-q climate and +20.6% (9.9 PgC/yr) for the GISS climate. The responses of global total carbon storage are +17.3% (157 PgC) for the MIT L-O climate, +18.3% (166 PgC) for GFDL-q climate and +19.5% (178 PgC) for the GISS climate. Among the three climate change predictions, distributions of cumulative NPP and total carbon storage along the 0.5° resolution latitudinal bands vary slightly, and there are only minor differences in cumulative NPP and total carbon storage for each of 18 biomes. Relatively large differences in NPP and total carbon storage among the three climate change predictions occur in individual grid cells at high latitudes of the northern hemisphere.

The results demonstrate that the 2-D climate model is appropriate and useful for impact assessment and uncertainty analysis within an integrated assessment framework at global and biome scales, given the compromise between computational efficiency in the 2-D climate model and more detailed spatial representation of climate fields in the 3-D GCMs.

1. INTRODUCTION

Atmospheric CO₂ concentration has increased since the pre-industrial era from about 280 ppmv to 356 ppmv (IPCC, 1994, 1995). The average rate of CO₂ concentration increase during the 1980s was 0.4% or 1.5 ppmv per year, which is equivalent to 3.2 GtC/yr, approximately 50% of total anthropogenic CO₂ emission (ibid.). There are large uncertainties about the path and magnitude of future anthropogenic emission of greenhouse gases, because of uncertainty in population growth, economic growth, technology development and other factors. These uncertainties, combined with uncertainties in natural biogeochemical cycles, lead to questions about the rate and magnitude of changes of concentrations of greenhouse gases (especially CO₂) in the atmosphere.

Increases in CO₂ and other greenhouse gases in the atmosphere will increase radiative forcing of climate. The resultant climate change combined with the increase of atmospheric CO₂ concentration may in turn have significant impacts on the structure and biogeochemistry of terrestrial ecosystems (Gates, 1985; Houghton and Woodwell, 1989; Melillo et al., 1990; Jenkinson et al., 1991). At the global and continental scales, a number of studies have investigated the potential impact of climate change and elevated CO₂ on primary production and carbon storage of natural ecosystems and managed ecosystems. One approach was to apply +1 °C, +2 °C or +4 °C temperature increase and/or ±10%, ±20% change of precipitation uniformly over a study area (Esser, 1987, 1990; Buol et al., 1990; Zhang, 1993; Potter et al., 1993; McGuire et al., 1993, 1995; Schimel et al., 1994; Melillo et al., 1995). This simple approach ignores potential differences in both latitudinal and longitudinal variations in temperature and precipitation. Another approach used climate outputs from 3-dimensional (3-D) atmospheric general circulation models (GCMs) for doubled CO₂ scenarios (Melillo et al., 1993; VEMAP Members, 1995; Parton et al., 1995; Rosenzweig and Parry, 1994). Outputs from these 3-D GCMs are commonly used: Goddard Institute for Space Studies (GISS; Hansen et al., 1983, 1984), Geophysical Fluid Dynamic Laboratory (GFDL; Manabe and Wetherald, 1987; Wetherald and Manabe, 1988), Oregon State University (OSU; Schlesinger and Zhao, 1989), and United Kingdom Meteorological Office (UKMO; Wilson and Mitchell, 1987). These climate outputs represent mostly equilibrium climate for doubled CO₂ scenarios.

Various climate change scenarios, resulting from different scenarios of anthropogenic emission of greenhouse gases and the corresponding atmospheric CO₂ concentrations, need to be explored in order to quantify impact and uncertainty of global climate change relative to policy and decision making (Jacoby and Prinn, 1994). The potential to apply 3-D GCMs in uncertainty analysis and impact assessment of climate change is limited, because of the substantial computational requirements of 3-D GCMs. By observing that latitudinal variations play a stronger role than longitudinal variations in determining climate, and that transport by large-scale 3-D eddies can be parameterized by using dynamical theory, a 2-dimensional climate model has been incorporated into the integrated assessment framework for climate change at the Massachusetts Institute of Technology (2-D MIT L-O climate model; see Yao and Stone, 1987; Stone and Yao, 1987, 1990; Sokolov and Stone, 1995). The 2-D MIT L-O climate model simulates the zonally averaged climate separately over land and ocean as a function of latitude and height. The model has 23 latitudinal bands, corresponding to a resolution of 7.826°, and 9 levels in the vertical dimension. The structure and parameterization have much in common with the 3-D GISS climate model (Hansen et al., 1983), however, the 2-D model runs 23 times faster than the GISS GCM with 8° (latitude) × 10° (longitude) resolution and 115 times faster than the GISS GCM with 4° × 5° resolution. These short run times of the 2-D model are an important characteristic for uncertainty analysis.

In this study, we ran a new version of Terrestrial Ecosystem Model (McGuire et al., 1995), driven by climate outputs from two 3-D GCMs and the 2-D MIT L-O climate model. Our objectives were: (1) to report the responses of primary production and carbon storage to climate change associated with an effective doubling of CO₂ for the new version of TEM; and (2) to examine the ecological consequences of climate change as represented by a 2-D climate model rather than a 3-D GCM. We examined the similarities and differences in the responses of net

primary production (NPP) and total carbon storage to different climate change predictions from the 2-D climate model and 3-D GCMs across various spatial scales (i.e., globe, latitudinal gradient, biome, grid cells, economic regions).

2. THE TERRESTRIAL ECOSYSTEM MODEL (TEM)

The TEM (Raich et al., 1991; McGuire et al., 1992; McGuire et al., 1993; McGuire et al., 1995) is a process-based ecosystem model that simulates important carbon and nitrogen fluxes and pools for various terrestrial ecosystems (Figure 1). It runs at a monthly time step. Driving variables include monthly climate (precipitation, mean temperature and mean cloudiness), soil texture (sand, clay and silt proportion), elevation, vegetation and water availability. The water balance model of Vorosmarty et al. (1988) is used to generate hydrological input (e.g., PET, soil moisture) for TEM. For global extrapolation, TEM uses spatially-explicit data sets that are gridded at a resolution of 0.5° latitude by 0.5° longitude (about 55 km × 55 km at the equator). The global data sets include long-term average climate data (Cramer, personal communication), potential vegetation (Melillo et al., 1993), soil texture (FAO/CSRC/MBL, undated) and elevation (NCAR/Navy, 1984). These data sets contain 62,483 land grid cells, including 3,059 ice grid cells and 1,525 wetland grid cells. Geographically, the global data sets cover land areas between 56 °S and 83 °N.

In this study, we used TEM version 4, which has a number of modifications to version 3 (Melillo et al., 1993). The TEM version 3 has been used to examine the response of NPP and carbon storage to changes in climate and atmospheric CO₂ concentration (McGuire et al., 1993; Melillo et al., 1993, 1994). The detailed descriptions of these TEM modifications are presented elsewhere (McGuire et al., 1995). Major modifications include changes in the algorithms describing: temperature effects on gross primary production, moisture effects on nitrogen uptake by plants and microbes, decomposition of soil organic matter, and the factors influencing the carbon to nitrogen ratio of vegetation in grasslands. In TEM version 4, soil texture is treated as a continuous variable based on proportion of silt plus clay, rather than a categorical variable with five classes (sand, sand loam, loam, clay loam, and clay). More model parameters now depend on soil texture, including the carbon and nitrogen uptake capacity of vegetation, the decomposition and immobilization capacity of microbes. Plant rooting depth, porosity, field capacity and wilting point are also dependent upon soil texture.

In this study, we focused on NPP and total carbon storage, which are two important variables in impact assessment. Total carbon storage is the sum of vegetation carbon and reactive soil organic carbon. NPP is calculated as the difference between gross primary productivity (GPP) and plant respiration (R_A). The flux R_A , which includes both maintenance respiration and construction respiration, is calculated at each monthly time step as a function of temperature and vegetation carbon. The flux GPP is calculated at each monthly time step as follows:

$$GPP = C_{max} f(PAR) f(LEAF) f(T) f(CO_2, H_2O) f(NA)$$

where C_{max} is the maximum rate of C assimilation, PAR is photosynthetically active radiation, LEAF is leaf area relative to maximum annual leaf area, T is temperature, CO_2 is atmospheric CO_2 concentration, H_2O is water availability, and NA is nitrogen availability (Raich et al., 1991).

3. CLIMATE CHANGE SCENARIOS AND ATMOSPHERIC CO_2 CONCENTRATION

We used climate outputs for $1 \times CO_2$ and $2 \times CO_2$ simulations from two 3-D GCMs, i.e., GISS (Hansen et al., 1983), GFDL-q (Wetherald and Manabe, 1988); and the 2-D MIT L-O climate model (Sokolov and Stone, 1995). The spatial resolution (longitude \times latitude) is $10.0^\circ \times 7.826^\circ$ for GISS and $7.5^\circ \times 4.44^\circ$ for GFDL-q. The climate outputs from GISS and GFDL-q were interpolated to $0.5^\circ \times 0.5^\circ$ grid cells by applying a spherical interpolation routine to the data (Willmott et al., 1985). We generated “future climate” by: (1) adding the absolute difference in temperature between $2 \times CO_2$ and $1 \times CO_2$ simulations to the contemporary temperature data; (2) multiplying the ratio in precipitation between $2 \times CO_2$ and $1 \times CO_2$ simulations to the contemporary precipitation data; and (3) multiplying the ratio in cloudiness between $2 \times CO_2$ and $1 \times CO_2$ simulations to the contemporary cloudiness data. For the 2-D MIT L-O climate, the absolute differences in temperature and the ratios of precipitation and cloudiness between the $2 \times CO_2$ and $1 \times CO_2$ simulations were calculated for each latitudinal band. We then applied the zonally averaged data to all the $0.5^\circ \times 0.5^\circ$ grid cells within the latitudinal band. By generating “future climate” in this way, we have assumed that general patterns of climate within a latitudinal band will remain unchanged. For the contemporary climate, the long-term monthly average data of precipitation, temperature and cloudiness from the Cramer and Leemans CLIMATE database (Cramer, personal comm.) were used. The Cramer and Leemans climate data are an improvement of the Leemans and Cramer (1990) climate data set, as the Cramer and Leemans climate data sets have many more weather stations and a new algorithm for spatial interpolation is used.

The GISS GCM and MIT L-O climate model simulated climate conditions for both “current” CO_2 ($1 \times CO_2$, 315 ppmv) and doubled “current” CO_2 ($2 \times CO_2$, 630 ppmv). Projected changes in global mean annual temperature vary little among the three climate models: $+4.2^\circ C$ for GISS, $+4.0^\circ C$ for GFDL-q, and $+4.2^\circ C$ for MIT L-O. Change of global annual precipitation ranges from $+8.3\%$ for GFDL-q, $+11.0\%$ for GISS, to $+11.5\%$ for MIT L-O. Projected decrease of global annual mean cloudiness are largest (-3.4%) for GISS, intermediate (-2.6%) for MIT L-O, and lowest (-0.7%) for GFDL-q. Figure 2 compares the zonal mean climate changes predicted by the 2-D MIT L-O model and 3-D GCMs. The GCMs outputs were also averaged over the same latitudinal bands as the those of the 2-D MIT L-O model. All three models predicted that increases of annual mean temperature are small in low latitudes but large in high latitudes (Figure 2a). As functions of latitude, there are large variations in percent changes of annual precipitation and annual mean cloudiness in the climate models (Figure 2b, 2c).

Atmospheric CO_2 concentration has increased since the pre-industrial period from about 280 ppmv in 1800, to 315 ppmv in 1957, and to 356 ppmv in 1993. The additional radiative forcing due to this CO_2 increase is $1.56 W/m^2$, accounting for approximately 63% of the total additional radiative forcing by the long-lived greenhouse gases (CO_2 , CH_4 , N_2O and halocarbons) (IPCC, 1994, 1995). Atmospheric concentrations of other greenhouse gases (e.g., CH_4 , N_2O , halocarbons) are also increasing. An “effective CO_2 doubling” has been defined as the combined radiative forcing of all greenhouse gases having the same forcing as doubled CO_2 (Rosenzweig

and Parry, 1994). According to the emission scenarios projected by the economic-emission model in the MIT integrated assessment framework, the radiative forcing from CO₂ accounts for about 76% of the total additional radiative forcing equivalent to a doubling of atmospheric CO₂ concentration (from 315 ppmv to 630 ppmv). Therefore, we used 522 ppmv CO₂ as the CO₂ change corresponding to an effective CO₂ doubling, instead of using 630 ppmv CO₂ to drive TEM.

Similarly, other studies have also projected that CO₂ is still the dominant long-lived greenhouse gas in the next century and that its added radiative forcing contributes between 76% and 84% of the total additional radiative forcing (IPCC, 1995). A number of experimental studies have shown that photosynthesis and water use efficiency of plants are enhanced under elevated CO₂ levels (Kimball, 1975; Idso and Kimball, 1993; Owensby et al., 1993; Polley et al., 1993; Idso and Idso, 1994). The results from a simulation of the TEM model have also shown that doubling atmospheric CO₂ alone can potentially increase global NPP and carbon storage (Melillo et al., 1993, 1995). The interaction between CO₂ and climate change also affects the responses of NPP and carbon storage (Melillo et al., 1993, 1995). Therefore, it is more appropriate to use an effective doubling of CO₂ when examining the responses of terrestrial ecosystems to changes in climate and atmospheric CO₂ concentration.

To determine responses to climate change with elevated CO₂, we ran TEM under: (1) contemporary climate with 315 ppmv CO₂, and (2) climate change with 522 ppmv CO₂. The TEM simulation driven by contemporary climate with 315 ppmv CO₂ is the baseline or reference. We ran TEM to its equilibrium state, i.e., all carbon and nitrogen fluxes are balanced within an ecosystems. Therefore, its estimates of carbon and nitrogen fluxes and pool sizes apply only to mature, undisturbed vegetation and ecosystems. Effects of land use and management on carbon and nitrogen dynamics were not considered.

4. RESULTS

4.1 NPP and total carbon storage under contemporary climate and 315 ppmv CO₂

For the contemporary climate with 315 ppmv CO₂, TEM estimated global annual NPP to be 47.9 PgC/yr (Table 1). Cumulative NPP in tropical regions is estimated to be as much as two times higher than cumulative NPP in temperate regions (Figure 3a). Tropical evergreen forests account for 34% of global NPP, although its area is about 14% of the global land area used in the simulations (Table 1). Tropical ecosystems (tropical evergreen forest, tropical deciduous forest, xeromorphic forest and tropical savanna) account for 57% of global NPP. Cumulative NPP is low in high latitude ecosystems in the northern hemisphere (Figure 3a), where NPP is primarily limited by low temperature and consequently low net nitrogen mineralization. Polar desert/alpine tundra and moist tundra ecosystems occur over 8% of the global land area but account for only 2% (0.9 PgC/yr) of global NPP (Table 1). Together, boreal forests and boreal woodlands account for 14.5% of the global land area and their annual NPP is about 8% (3.9 PgC/yr) of global NPP. In arid regions (arid shrubland and desert), NPP is limited by water availability. Cumulative NPP in

arid regions accounts for 4% of global NPP, although the area of arid regions is about 20% of the global land area.

Table 1. Resonse of annual net primary production and total carbon storage to changes in climate and atmospheric CO₂ concentration.

Vegetation type	Climate Scenarios: grid # area (km ²)		Annual Net Primary Production				Total Carbon Storage			
			CO ₂ level:		522 ppmv		315 ppmv		522 ppmv	
			315 ppmv	Contemp	MIT L-0	GISS	GFDL-q	Contemp	MIT L-0	GISS
		(Pg C/yr)	(%)	(%)	(%)	(Pg C)	(%)	(%)	(%)	
Polar desert/alpine tundra	3,578	5.3E+6	0.3	25.5	30.7	29.7	36	-2.5	2.3	1.6
Wet/moist tundra	4,207	5.2E+6	0.5	25.3	31.7	30.5	63	-5.7	0.8	-0.3
Boreal forest	7,577	1.2E+8	2.8	20.1	25.0	26.8	251	4.8	11.0	11.2
Boreal woodland	4,545	6.5E+6	1.0	20.6	29.7	29.3	101	-3.9	7.8	7.1
Temperate mixed forest	2,320	5.2E+6	3.0	20.5	21.6	20.1	114	11.7	12.2	10.2
Temperate coniferous forest	1,126	2.5E+6	1.0	22.6	21.0	22.0	43	11.9	9.3	10.1
Temperate deciduous forest	1,666	3.7E+6	2.4	21.1	23.0	22.6	92	12.3	13.3	12.4
Tall grassland	1,567	3.6E+6	1.2	21.5	28.0	24.0	18	0.5	1.5	-0.7
Short grassland	2,067	4.7E+6	1.0	24.1	29.0	27.7	20	1.6	1.3	-0.3
Tropical savanna	4,666	1.4E+7	5.7	14.7	21.1	15.0	124	6.8	8.3	5.9
Arid shrubland	5,784	1.5E+7	1.5	30.1	33.5	25.3	33	8.4	6.5	0.8
Tropical evergreen forest	5,868	1.8E+7	16.3	14.2	15.5	13.6	467	9.4	8.7	9.0
Tropical deciduous forest	1,607	4.7E+6	2.8	12.7	15.0	13.7	82	7.1	7.4	8.0
Xeromorphic forest	2,387	6.9E+6	2.4	21.4	23.7	19.5	49	7.7	4.8	4.8
Desert	4,170	1.2E+7	0.4	36.5	41.5	28.0	7	16.0	15.2	4.2
Temperate savanna	2,921	6.8E+6	2.4	21.5	25.0	23.7	74	9.7	11.1	8.8
Mediterranean shrubland	575	1.5E+6	0.4	22.9	27.3	22.0	11	5.8	7.0	2.4
Temperate broadleaf evergreen forest	1,268	3.3E+6	2.8	17.4	16.7	20.3	74	10.5	7.8	11.9
Total	57,899	1.3E+8	47.9	17.8	20.6	18.5	1,659	6.9	8.7	8.2

The TEM estimated total terrestrial carbon storage (vegetation carbon plus reactive soil organic carbon) of the globe to be 1659 PgC (Table 1), including 909 PgC of vegetation carbon and 750 PgC of reactive soil organic carbon. Total carbon storage has a bimodal distribution across latitude with the highest storage in both tropical zone in the southern hemisphere and high latitudes in the northern hemisphere (Figure 3b). About 43% of global total carbon storage occurs in tropical ecosystems, where most of the carbon is stored in vegetation. Of the 18 biomes, tropical evergreen forest accounts for the largest portion (about 28%) of global total carbon storage (Table 1). Total carbon storage of polar desert/alpine tundra and moist/wet tundra is 100 PgC, about 6% of global total carbon storage. Boreal forest and boreal woodlands account for about 21% (351 PgC) of global total carbon storage. A large proportion of carbon in high latitudes is stored as soil organic carbon. Because of low temperatures in temperate and high latitudes, soil organic matter decomposes slowly and has accumulated over centuries.

4.2 Response of NPP to climate change and elevated CO₂

The TEM estimated that global NPP increases substantially for climate change with 522 ppmv CO₂ but varies little among the three climate change predictions: +17.8% (8.6 PgC/yr) for the MIT L-O climate, +18.5% (8.9 PgC) for the GFDL-q climate, and +20.6% (9.9 PgC) for the GISS climate (Table 1). Along the 0.5° resolution latitudinal gradient, the response of cumulative NPP has a bimodal distribution with the largest increases in both tropical forest regions and the temperate ecosystems in the northern hemisphere (Figure 4a). Generally, the latitudinal distribution of NPP change under the MIT L-O climate is similar to those under the GISS and GFDL-q climate, except for relatively large differences within the 50.5 °N to 58.5 °N and 66.5 °N to 74 °N bands (Figure 4a). The projected change in annual cloudiness within the 50.5 °N to 58.5 °N band is over 20% higher in the MIT L-O predictions than in the GISS and GFDL-q predictions (Figure 2c). Higher cloudiness reduces photosynthetic active radiation, which in turn results in reduced gross primary productivity. Projected changes in mean annual cloudiness and mean annual temperature by the MIT L-O model were over 10% and 2 °C higher than those by the GISS and GFDL-q models within the 66.5 °N to 74 °N band.

Cumulative NPP for each of the 18 biomes increases considerably (Table 1). Percent NPP increase is higher in arid ecosystems than in temperate and tropical forest ecosystems. The NPP of arid ecosystems is primarily limited by water. Elevated atmospheric CO₂ concentration would enhance water use efficiency of plants. Temperate and high latitude ecosystems are generally nutrient-limiting systems. Increased temperature and precipitation would result in a higher rate of decomposition of soil organic matter. As a result, more nitrogen is released from the soil to be available for plant uptake.

Cumulative NPP for most of the 18 biomes varies only slightly among the three climate change predictions (Table 1). The NPP responses in the high latitude regions (boreal forest, boreal woodland, wet/moist tundra, polar desert/alpine tundra) under the MIT L-O climate are 4 to 9% lower than those under the GISS and GFDL-q climate. This is mostly attributable to the relatively larger increases of temperature and cloudiness in the high latitude regions, as projected by the MIT L-O model (Figure 2a).

At the grid cell scale, the means of annual NPP for each of the 18 biomes increase considerably, but vary little among the three climate change predictions (Table 2). The differences in means of annual NPP between the 2-D MIT L-O climate and the 3-D GISS and GFDL-q climate range from ±(7 to 8)% for boreal woodland to ±(4 to 6)% for tundra and boreal forest to within ±1% for the other biomes. Also, the standard deviations of annual NPP for each of the 18 biomes vary little among the three climate change predictions (Table 2).

4.3 Response of total carbon storage to climate change and elevated CO₂

For climate change with 522 ppmv CO₂, TEM estimated that the increase of global total carbon storage varies from +6.9% (115 PgC) for the MIT L-O climate, to +8.2% (137 PgC) for the GFDL-q climate, to +8.7% (144 PgC) for the GISS climate (Table 1). The responses vegetation carbon and soil organic carbon differ significantly from each other. Global vegetation carbon increases substantially: +17.3% (157 PgC) for the MIT L-O climate, +18.3% (166 PgC)

for the GFDL-q climate, and +19.5% (178 PgC) for the GISS climate. In contrast, the pool of reactive soil organic carbon decreases moderately, i.e., -5.6% (42 PgC) for the MIT L-O climate, -4.4% (33 PgC) for the GISS climate, and -4.0% (30 PgC) for the GFDL-q climate.

Table 2. Mean and standard deviation of annual net primary production under various climate scenarios and CO₂ levels.

Vegetation type	CO ₂ level: 315 ppmv		522 ppmv					
	Climate Scenarios: Contemporary		MIT L-O		GISS		GFDL-q	
	mean [†] (gC/m ² /yr)	stddev	mean (gC/m ² /yr)	stddev	mean (gC/m ² /yr)	stddev	mean (gC/m ² /yr)	stddev
Polar desert/alpine tundra	62	24	77	27	81	29	80	28
Wet/moist tundra	103	29	129	32	135	31	134	33
Boreal forest	228	36	274	48	285	41	389	43
Boreal woodland	157	31	189	38	204	37	203	34
Temperate mixed forest	570	117	686	127	693	133	684	135
Temperate coniferous forest	397	126	487	138	481	129	484	142
Temperate deciduous forest	661	108	800	116	812	126	810	130
Tall grassland	330	166	401	192	423	207	409	186
Short grassland	221	71	274	84	284	89	281	80
Tropical savanna	411	183	472	206	498	217	473	207
Arid shrubland	99	41	128	53	132	52	124	50
Tropical evergreen forest	916	183	1046	224	1059	217	1041	219
Tropical deciduous forest	588	209	663	238	676	236	669	230
Xeromorphic forest	354	182	430	209	438	208	423	208
Desert	34	28	47	36	49	38	44	34
Temperate savanna	348	131	423	156	435	154	430	154
Mediterranean shrubland	304	130	373	158	386	155	370	151
Temperate broadleaf evergreen forest	828	235	973	243	966	244	996	248
Globe	368	292	434	334	444	336	436	333

[†] mean: average NPP, weighed by area of pixels; stddev: standard deviation

Along the 0.5° resolution latitudinal gradient, the response of total carbon storage has a bimodal distribution with the largest increase in the northern temperate regions and tropical regions (Figure 4b). The response of total carbon storage under the MIT L-O climate is similar to the responses of total carbon storage under the GISS and GFDL-q climate, except for the large difference within the 50.5 °N to 58.5 °N and 66.5 °N to 74.0 °N bands. Within these two latitudinal bands, the MIT L-O model projects relatively higher temperature and cloudiness than the GISS and GFDL-q models. Higher temperature increases loss of soil organic carbon, while higher cloudiness results in a decrease in the response of vegetation carbon due to lower annual NPP.

Responses of total carbon storage for most of the 18 biomes are similar among the three climate change predictions. For the GISS climate, total carbon storage increases from 0.5% in wet/moist tundra to 15.2% in desert (Table 1). For the MIT L-O climate, the response of total carbon storage ranges from a decrease of 6.0% in wet/moist tundra to an increase of 16.0% in desert. For the GFDL-q climate, the increase of total carbon storage ranges from 0.8% in arid

shrubland to 4.2% in desert, which is a much lower range than those for the GISS and MIT L-O climate.

At the grid cell scale, the means of total carbon storage for each of the 18 biomes vary to some degree among the three climate change predictions (Table 3). The differences in the means of total carbon storage between the 2-D MIT L-O climate model and the 3-D GCMs climate models range from $\pm(11$ to $12)\%$ for boreal woodland, to $\pm(5$ to $7)\%$ for tundra and boreal forest, to within $\pm 2\%$ for the other biomes. Also, the standard deviations of total carbon storage for each of the 18 biomes vary little among the three climate change predictions (Table 3).

Table 3. Mean and standard deviation of total carbon storage under various climate scenarios and CO₂ levels.

Vegetation type	CO ₂ level: 315 ppmv		522 ppmv					
	Contemporary		MIT L-O		GISS		GFDL-q	
	mean [†] (gC/m ² /yr)	stddev	mean (gC/m ² /yr)	stddev	mean (gC/m ² /yr)	stddev	mean (gC/m ² /yr)	stddev
Polar desert/alpine tundra	6,890	2,042	6,711	1,987	7,041	2,087	6,995	2,093
Wet/moist tundra	12,112	2,299	11,388	2,231	12,178	2,109	12,043	2,095
Boreal forest	20,096	2,487	21,050	3,683	22,299	2,501	22,341	2,799
Boreal woodland	15,597	2,296	14,995	2,874	16,816	2,485	16,710	2,306
Temperate mixed forest	21,636	3,211	24,174	3,539	24,266	3,519	23,851	3,781
Temperate coniferous forest	17,412	3,905	19,466	4,143	19,008	3,984	19,159	4,349
Temperate deciduous forest	25,122	3,417	28,223	3,641	28,463	3,755	28,243	4,033
Tall grassland	4,962	1,542	4,985	1,506	5,036	1,503	4,929	1,457
Short grassland	4,339	1,170	4,397	1,160	4,381	1,169	4,313	1,185
Tropical savanna	8,942	3,672	9,554	3,877	9,685	3,867	9,467	3,857
Arid shrubland	2,272	1,431	2,463	1,504	2,421	1,476	2,291	1,426
Tropical evergreen forest	26,267	5,121	28,745	6,007	28,559	5,713	28,625	5,904
Tropical deciduous forest	17,402	6,441	18,644	6,970	18,683	6,696	18,790	6,736
Xeromorphic forest	7,129	4,022	7,680	4,121	7,468	3,957	7,468	4,068
Desert	577	647	669	687	664	693	601	637
Temperate savanna	10,792	4,331	11,834	4,612	11,991	4,595	11,738	4,730
Mediterranean shrubland	7,401	3,365	7,833	3,530	7,916	3,406	7,577	3,393
Temperate broadleaf evergreen forest	22,302	5,195	24,634	5,142	24,049	5,007	24,967	5,203
Globe	12,728	8,779	13,609	9,651	13,835	9,681	13,777	9,773

[†] mean: average carbon storage, weighed by area of pixels; stddev: standard deviation

5. DISCUSSION

5.1 Contemporary climate, NPP and total carbon storage

A number of studies have estimated global NPP under contemporary climate, using either extrapolation of field data or modeling approaches. For the thirteen estimates of global NPP summarized by Melillo (1994), global NPP has a mean of 57 PgC/yr and a standard deviation of 17.4 PgC/yr. Our estimate of global NPP (47.9 PgC/yr) under contemporary climate with 315

ppmv CO₂ is very close to the estimate (48.2 PgC/yr) by Whittaker and Likens (1973). Potter et al. (1993) estimated 48 PgC/yr of global NPP, using remote sensing data in 1987 and climate data.

The global NPP estimate (47.9 PgC/yr) in this study is slightly lower than the estimate (51.0 PgC/yr) in one earlier study (Melillo et al., 1993), which used TEM version 3, precipitation and temperature data from Legates and Willmott (1988), and cloudiness data from Hahn et al. (1988). In general, the Cramer and Leemans climate data used in this study represent a cooler, drier and sunnier world than data from Legates and Willmott (1988) and Hahn et al. (1988). For the Cramer and Leemans climate dataset, global average annual mean temperature, annual precipitation and cloudiness over lands are 12.8 °C, 795 mm, and 46%, respectively. The Legates and Willmott dataset has a global mean annual temperature of 13.8 °C, and global average annual precipitation of 845 mm, while the Hahn dataset has a global average annual cloudiness of 56%. The differences in temperature and precipitation between the Cramer and Leemans dataset and Legates and Willmott dataset are relatively small in tropical regions but large in temperate and high latitudes.

The estimate of global total carbon storage (1659 PgC) in this study is also lower than the estimate (1810.5 PgC) in an earlier study using TEM version 3 (Melillo et al., 1995). Global reactive soil organic carbon estimated by TEM (750 PgC) in this study is about 50% of the approximately 1500 PgC estimated by several inventories of soil organic carbon to 1 meter depth (Schlesinger, 1977; Post et al., 1982; Eswaran et al., 1993). Because of the latitudinal distributions of vegetation carbon and reactive soil organic carbon, as well as the latitudinal gradients of temperature change, the response of total carbon storage to climate change may be dominated by vegetation in tropical regions but by soils in temperate and high latitude areas.

5.2 Future climate, NPP and total carbon storage

The responses of global NPP to climate change with 522 ppmv CO₂ in this study are slightly lower than those in an earlier study (Melillo et al., 1993), in which global NPP response was estimated to be +25.1% for the GFDL-q climate, and 25.9% for the GISS climate. The difference is mainly due to the larger increase of CO₂ concentration (from 312.5 ppmv to 625 ppmv) used in the earlier study (Melillo et al., 1993). The responses of NPP and total carbon storage to climate change with 522 ppmv CO₂ have a bimodal distributions along the 0.5° resolution latitudinal gradient. This suggests that tropical regions and northern temperate regions may be the two net sinks of terrestrial carbon storage with respect to ecosystem metabolism. The tropical sink of carbon may offset to some degree the carbon loss caused by land use change in tropical regions, e.g., deforestation.

The simulation results showed that TEM-estimated NPP and total carbon storage responses for the 2-D MIT L-O and the 3-D GCMs (GISS and GFDL-q) climate change calculations are quite similar to each other on the biome and globe scales. TEM-estimated carbon flux and storage for the 2-D MIT L-O climate are slightly closer to those for the GFDL-q climate than to those for the GISS climate, although the 2-D MIT L-O climate model was developed from the 3-D GISS climate model. The differences in estimates of responses of NPP and total carbon storage between the 2-D MIT L-O and the 3-D GCMs climate change predictions are much smaller than the responses of NPP and total carbon storage to climate change and elevated atmospheric CO₂ concentration.

Therefore, use of the climate change predictions by the 2-D MIT L-O climate model for impact assessment and uncertainty analysis would generally provide almost equally useful information on the responses of terrestrial primary production and carbon storage on the global and biome scales as the 3-D GCMs provide.

The largest differences in estimates of NPP and total carbon storage between the 2-D MIT L-O climate and the 3-D GISS and GFDL-q climate occur in high latitudes in the northern hemisphere, where vegetation is dominated by tundra and boreal forest and woodland. Global warming is very likely to result in shrinkage of tundra and northward expansion of boreal and temperate ecosystems (Emanuel et al., 1985; Woodward and McKee, 1991; Cramer and Leemans, 1993). The predictions of climate changes in high latitudes are sensitive to the representation of the ocean and sea ice, and in particular, there is considerable uncertainty as to what is the correct way to parameterize sea ice in climate models. Further work is underway to modify the 2-D MIT L-O climate model for improving its projection of climate change in high latitudes in the northern hemisphere.

At the scale of grid cells, maps of annual NPP and total carbon storage showed that spatial distributions of NPP and total carbon storage under the 2-D MIT L-O and 3-D GISS and GFDL-q climate change predictions disagree to some degree, particularly in high latitude regions. In simple linear regressions for each of the 18 biomes, the regression coefficients (r^2 , slope, and intercept) for percent responses of NPP between the 2-D MIT L-O climate and either of the two 3-D GCMs climate are similar to the regression coefficients between the two 3-D GCMs climate. The situation is the same for total carbon storage. The 2-D climate model should not be applied for regional studies, as it represents only the zonal average climate over land or ocean and has no longitudinal variations. For studies with objectives of examining responses of NPP and total carbon storage to climate change on regional and grid cell scales, 3-D climate models are more appropriate.

5.3 Policy making, NPP and carbon storage

In relation to policy making, spatial aggregations of NPP and carbon storage responses for the economic regions would provide an important linkage between the projection of anthropogenic emission of trace gases, their impacts on terrestrial ecosystems and the subsequent feedback on economic performance. The economic-emission model in the MIT Integrated Framework, which is based on the OECD General Equilibrium Environmental model (see OECD, 1992), divides the world into 12 economic regions. The model projects economic development and associated anthropogenic emissions of greenhouse gases in the 12 economic regions.

Annual NPP increases substantially for each of the 12 economic regions and varies little among the three climate change predictions (Table 4). For most economic regions, the responses of annual NPP are slightly smaller under the MIT L-O climate than under the GISS and GFDL-q climate. India, the Dynamic Asian countries (e.g., South Korea, Thailand, Singapore) and energy exporting countries (e.g., Egypt, Congo, Mexico, Iran, Iraq) have relatively smaller responses of annual NPP. Similarly, the responses of total carbon storage are also close to each other among the three climate change predictions for most economic regions. An exception is the former Soviet Union economic region, where total carbon storage decreases slightly (-0.6%) under the 2-D MIT L-O climate, but increase 8.0% under the GFDL-q climate and 9.0% under the GISS climate

(Table 4). As described earlier, this difference is caused by the higher temperature and cloudiness in the high latitudes in the MIT L-O climate. These comparisons indicate that the 2-D MIT L-O climate model is also appropriate for impact assessment at the scale of the economic regions.

Table 4. Economic regional responses of annual net primary production and total carbon storage to changes in climate and atmospheric CO₂ concentrations.

Economic regions	Climate Scenarios: grid # area (km ²)		Annual Net Primary Production				Total Carbon Storage			
			CO ₂ level:		522 ppmv		315 ppmv		522 ppmv	
			315 ppmv	Contemp (Pg C/yr)	MIT L-0 (%)	GISS (%)	GFDL-q (%)	Contemp (Pg C)	MIT L-0 (%)	GISS (%)
USA	4,322	9.1E+6	3.2	22.6	23.3	20.0	118	9.1	9.2	5.6
Japan	163	4.0E+5	0.3	21.7	20.4	28.6	9	12.5	12.2	17.4
India	1,089	3.1E+6	1.2	11.6	15.3	17.6	35	6.0	8.0	10.4
China	3,807	9.4E+6	3.6	17.9	18.6	23.1	131	8.8	7.7	11.6
Brazil	2,726	8.2E+6	6.3	15.9	16.9	14.8	6	15.9	16.9	14.8
EEC (European Community)	1,109	2.4E+6	1.3	23.6	23.5	22.6	45	13.5	13.2	11.2
EET (Eastern European Countries)	552	1.1E+6	0.6	24.6	24.4	20.8	22	13.8	13.1	9.7
DAE (Dynamic Asia Economic)	330	9.6E+5	0.8	11.2	11.4	12.5	22	6.7	5.9	8.1
OOE (Other OECD Countries)	10,841	2.0E+7	4.7	23.2	25.1	22.7	231	7.1	8.6	8.0
FSU (Former Soviet Union)	13,467	2.1E+7	4.2	20.8	28.0	28.1	296	-0.6	9.0	8.0
EEX (Energy Exporting Countries)	7,847	2.2E+7	9.4	15.9	19.2	15.7	255	9.1	9.4	8.7
ROW (The Rest of the World)	11,646	3.2E+7	12.4	16.0	19.8	15.7	330	7.6	7.9	6.6

The good agreement in the estimates of NPP and total carbon storage responses between the 2-D MIT L-O climate and the 3-D GISS and GFDL-q climate may be attributed in part to the concept and formulation of TEM model and in part to the magnitude of changes in temperature, precipitation and cloudiness projected by these three climate models. In a recent ecosystem model comparison study, TEM, CENTURY (Parton et al., 1987; Parton et al., 1988; Parton et al., 1993) and Biome-BGC (Running and Coughlan, 1988; Running and Gower, 1991) gave quite different estimates of responses of NPP and total carbon storage for the conterminous United States, driven by the same data sets for climate change and elevated CO₂ levels (VEMAP Members, 1995). For climate change with 710 ppmv CO₂ (GFDL R30), responses of total NPP in the conterminous U.S. is +20.2% for Biome-BGC, +22.1% for CENTURY, and +30.5% for TEM. In contrast, the response of total carbon storage varies considerably: -11.0% for Biome-BGC, +6.1% for CENTURY, and 14.6% for TEM (VEMAP Members, 1995). These ecosystem models have different sensitivities to changes in temperature, precipitation, cloudiness and CO₂ level.

In a study using alternative input datasets of climate, solar radiation and soil texture for the conterminous U.S. to drive TEM, the results shows that NPP estimates are sensitive to the different input datasets, partly dependent upon the magnitude of differences among the data sets (Pan et al., 1995). What are the relative roles of projected changes in temperature, precipitation and cloudiness to the overall responses of NPP and total carbon storage to climate change? We have completed a model sensitivity exercise with the aim of determining the relative contributions of

elevated CO₂ and projected changes of temperature, precipitation and cloudiness, using TEM. The results will be presented in a following paper.

6. ACKNOWLEDGEMENTS

The Terrestrial Ecosystem Model is part of the modeling framework for integrated assessment of climate change at the Massachusetts Institute of Technology. This study was supported by the MIT Joint Program on the Science and Policy of Global Change (CE-S-462041), DOE NIGEC (No:901214-HAR) and NASA EOS (NAGW-2669). We thank Ronald G. Prinn, Henry D. Jacoby, Richard S. Eckaus, Yude Pan and other colleagues in the MIT Joint Program for valuable discussions and comments.

7. REFERENCES

- Buol, S.W., P.A. Sanchez, J.M. Kimble and S.B. Weed, 1990, Predicted impact of climate warming on soil properties and use, *in*: "Impact of Carbon Dioxide, Trace Gases, and Climate Change on Global Agriculture," B.A. Kimball et al. (eds.), *ASA Special Publ.*, **53**:71-82.
- Cramer, W.P. and R. Leemans, 1993, Assessing impacts of climate change on vegetation using climate classification systems, *in*: "Vegetation Dynamics and Global Change," A.M. Solomon and H.H. Shugart (eds.), Chapman and Hall, New York, pp. 191-217.
- Emanuel, W.R., H.H. Shugart and M.P. Stevenson, 1985, Climatic change and the broad-scale distribution of terrestrial ecosystem complexes, *Climatic Change*, **7**:29-43.
- Esser, G., 1987, Sensitivity of global carbon pools and fluxes to human and potential climate impact, *Tellus*, **39B**:245-260.
- Esser, G., 1990, Modeling global terrestrial sources and sinks of CO₂ with special reference to soil organic matter, *in*: "Soils and Greenhouse Effect," A.F. Bouwman (ed.), John Wiley, New York, pp. 247-262.
- Eswaran, H., E. Van Der Berg and P. Reich, 1993, Organic carbon in soils of the world, *Soil Science Society of America*, **57**:192-194.
- FAO/CSRC/MBL, (undated), "Soil Map of the World, 1:5,000,000," Unesco, Paris, France. Digitization (0.5° resolution) by Complex Systems Research Center, University of New Hampshire, Durham, and modifications by Marine Biological Laboratory, Woods Hole.
- Gates, D.M., 1985, Global biospheric response to increasing atmospheric carbon dioxide concentration, *in*: "Direct Effect of Increasing Carbon Dioxide on Vegetation," B.R. Strain and J.D. Cure (eds.), DOE/ER-0238, U.S. Department of Energy, Washington, D.C.
- Hahn, J., S.G. Warren, J. London and J.L. Roy, 1988, "Climatological Data for Clouds over the Globe from Surface Observation," U.S. Department of Energy, Oak Ridge, Tennessee.
- Hansen, J., G. Russel, D. Rind, P. Stone, A. Lacis, S. Lebedeff, R. Ruedy and L. Travis, 1983, Efficient three dimensional global models for climate studies: Model I and II, *Monthly Weather Review*, **111**:609-662.
- Hansen, J., A. Lacis, D. Rind, G. Russel, P. Stone, I. Fung, R. Ruedy and J. Lerner, 1984, Climate sensitivity: Analysis of feedback mechanisms, *in*: "Climate Process and Climate Sensitivity," J.E. Hansen and T. Takahashi (eds.), *Geophysical Monograph 29*, Maurice Ewing series 5, American Geophysical Union, Washington, D.C., pp. 130-163.

- Houghton, R.A. and G.M. Woodwell, 1989, Global climatic change, *Scientific American*, **260**:36-47.
- Idso, S.B. and B.A. Kimball, 1993, Tree growth in carbon dioxide enriched air and its implications for global carbon cycling and maximum levels of atmospheric CO₂, *Global Biogeochemical Cycles*, **8**:537-555.
- Idso, K.E. and S.B. Idso, 1994, Plant responses to atmospheric CO₂ enrichment in the face of environmental constraints: A review of the last 10 years' research, *Agricultural and Forest Meteorology*, **69**:153-203.
- IPCC, 1994, "IPCC WGI Report: Radiative Forcing of Climate Change," Intergovernmental Panel on Climate Change, WMO/UNEP, Geneva, p. 5.
- IPCC, 1995, "Climate Change 1994: Radiative Forcing of Climate Change and an Evaluation of the IPCC IS92 Emission Scenarios," Intergovernmental Panel on Climate Change, Cambridge University Press, New York, pp. 196-197.
- Jacoby, H.D. and R.G. Prinn, 1994, "Uncertainty in Climate Change Policy Analysis," MIT Joint Program on the Science and Policy of Global Change, Report 1, MIT, 34 pgs.
- Jenkinson, D.S., D.E. Adams and A. Wild, 1991, Model estimate of CO₂ emissions from soil in response to global warming, *Nature*, **351**:304-306.
- Kimball, B.A., 1975, Carbon dioxide and agricultural yield: An assemblage and analysis of 430 prior observations, *Agronomy*, **75**:779-788.
- Leemans, R. and W.P. Cramer, 1990, "The IIASA Climate Database for Land Areas on a Grid with 0.5° Resolution," WP-90-41, International Institute for Applied Systems Analysis (IIASA), Laxenburg, Austria, 60 pgs.
- Legates, D.R. and C.J. Willmott, 1988, "Global Air Temperature and Precipitation Data Archive," Department of Geography, University of Delaware, Newark, Delaware.
- Manabe, S. and R.T. Wetherald, 1987, Large scale changes in soil wetness induced by an increase in carbon dioxide, *J. of Atmospheric Sciences*, **44**:1211-1235.
- McGuire, A.D., J.M. Melillo, D.W. Kicklighter and L.A. Joyce, 1995, Equilibrium responses of soil carbon to climate change: Empirical and process-based estimates, *Global Ecology and Biogeography Letters* (in press).
- McGuire, A.D., L.A. Joyce, D.W. Kicklighter, J.M. Melillo, G. Esser and C.J. Vorosmarty, 1993, Productivity response of climax temperate forests to elevated temperature and carbon dioxide: A North America comparison between two global models, *Climatic Change*, **24**:287-310.
- McGuire, A.D., J.M. Melillo, L.A. Joyce, D.W. Kicklighter, A.L. Grace, B. Moore III and C.J. Vorosmarty, 1992, Interactions between carbon and nitrogen dynamics in estimating net primary productivity for potential vegetation in North America, *Global Biogeochemical Cycles*, **6**(2):101-124.
- Melillo, J.M., 1994, Modeling land-atmospheric interaction: A short review, *in*: "Changes in Land Use and Land Cover: A Global Perspective," W.B. Meyer and B.L. Turner (eds), Cambridge University Press, pp. 387-409.
- Melillo, J.M., T.V. Callaghan, F.I. Woodward, E. Salati and S.K. Sinha, 1990, Climate change effects on ecosystems, *in*: "Climatic Change: The IPCC Scientific Assessment," J.T. Houghton, G.J. Jenkins and J.J. Ephraums (eds.), Cambridge University Press, New York, pp. 282-310.
- Melillo, J.M., A.D. McGuire, D.W. Kicklighter, B. Moore III, C.J. Vorosmarty and A.L. Schloss, 1993, Global climate change and terrestrial net primary production, *Nature*, **363**:234-240.
- Melillo, J.M., D.W. Kicklighter, A.D. McGuire, W.T. Peterjohn and K.M. Newkirk, 1995, Global change and its effects on soil organic carbon stocks, *in*: "Role of Nonliving Organic

- Matter in the Earth's Carbon Cycle," R.G. Zepp and C. Sonntag (eds.), John Wiley and Sons Ltd., pp. 175-189.
- NCAR/NAVY, 1984, "Global 10-minute Elevation Data," digital tape available through National Oceanic and Atmospheric Administration, National Geophysical Data Center, Boulder, Colorado.
- OECD, 1992, "The Economic Costs of Reducing CO₂ Emissions," OECD Economic Studies No. 19, OECD, Paris, France, 209 pgs.
- Owensby, C.E., P.I. Coyne, J.M. Ham, L.M. Auen and A.K. Knapp, 1993, Biomass production in a tallgrass prairie ecosystem exposed to ambient and elevated CO₂, *Ecological Applications*, **3**:644-653.
- Pan, Y., A.D. McGuire, D.W. Kicklighter and J.M. Melillo, 1995, The effect of climate and soil data on estimates of net primary production: A sensitivity analysis with the Terrestrial Ecosystem Model, *Global Change Biology* (in review).
- Parton, W.J., D.S. Schimel, C.V. Cole and D.S. Ojima, 1987, Analysis of factors controlling soil organic matter levels in Great Plain grasslands, *Soil Science Society of America*, **51**:1173-1179.
- Parton, W.J., J.W.B. Stewart and C.V. Cole, 1988, Dynamics of C, N, P and S in grassland soils: A model, *Biogeochemistry*, **5**:109-131.
- Parton, W.J., J.M.O. Scurlock, D.S. Ojima, T.G. Gilmanov, R.J. Scholes, D.S. Schimel, T.B. Kirchner, J.C. Menaut, T. Seastedt, E. Garcia Moya, A. Kamnalrut and J.I. Kinyamario, 1993, Observation and modeling of biomass and soil organic matter dynamics for the grassland biome worldwide, *Global Biogeochemistry Cycles*, **7**(4):785-809.
- Parton, W.J., J.M.O. Scurlock, D.S. Ojima, D.S. Schimel, D.O. Hall and SCOPE GRAM group members, 1995, Impact of climate change on grassland production and soil carbon worldwide, *Global Change Biology*, **1**:13-22.
- Polley, H.W., H.B. Johnson, B.D. Marino and H.S. Mayeux, 1993, Increase in C₃ plant water use efficiency and biomass over Glacial to present CO₂ concentrations, *Nature*, **361**:61-63.
- Post, W.M., W.R. Emanuel, P.J. Zinke and A.G. Stangenberger, 1982, Soil carbon pools and world life zones, *Nature*, **298**:156-159.
- Potter, C.S., J.T. Randerson, C.B. Field, P.A. Matson, P.M. Vitousek, H.A. Mooney and S.A. Klooster, 1993, Terrestrial ecosystem production: A process model based on global satellite and surface data, *Global Biogeochemical Cycles*, **7**:811-841.
- Raich, J. W., E.B. Rastetter, J.M. Melillo, D.W. Kicklighter, P.A. Steudler, B.J. Peterson, A.L. Grace, B. Moore III and C.J. Vorosmarty, 1991, Potential net primary productivity in South America: Application of a global model, *Ecological Applications*, **1**(4):399-429.
- Rosenzweig, C. and M.L. Parry, 1994, Potential impact of climate change on world food supply, *Nature*, **367**(13):133-138.
- Running, S.W. and J.C. Coughlan, 1988, A general model of forest ecosystem processes for regional applications. Part I. Hydrological balance, canopy gas exchange and primary production processes, *Ecological Application*, **42**:125-154.
- Running, S.W. and S.T. Gower, 1991, FOREST-BGC, a general model of forest ecosystem processes for regional applications. Part II. Dynamic carbon allocation and nitrogen budgets, *Tree Physiology*, **9**:147-160.
- Schimel, D.S., B.H. Braswell, E.A. Holland, R. McKeown, D.S. Ojima, T.H. Painter, W.J. Parton and A.R. Townsend, 1994, Climatic, edaphic and biotic controls over storage and turnover of carbon in soils, *Global Biogeochemical Cycles*, **8**(3):279-293.
- Schimel, D.S., W.J. Parton, T.G.F. Kittel, D.S. Ojima and C.V. Cole, 1990, Grassland biogeochemistry: Links to atmospheric processes, *Climatic Change*, **17**:13-25.

- Schlesinger, M.E. and Z. Zhao, 1989. Seasonal climatic changes induced by doubled CO₂ as simulated by the OSU atmospheric GCM/mixed-layer ocean model, *J. of Climate*, **2**:459-495.
- Schlesinger, W.H., 1977, Carbon balance in terrestrial detritus, *Annual Review of Ecology and Systematics*, **8**:51-81.
- Sokolov, A.P. and P.H. Stone, 1995, "Description and Validation of the MIT Version of the GISS 2-D Model," MIT Joint Program on the Science and Policy of Global Change, Report 2, MIT, 46 pgs.
- Stone, P.H. and M.S. Yao, 1987, Development of a two-dimensional zonally averaged statistical-dynamical model. Part II. The role of eddy momentum fluxes in the general circulation and their parameterization, *J. of Atmospheric Sciences*, **44(24)**:3769-3786.
- Stone, P.H. and M.S. Yao, 1990, Development of a two-dimensional zonally averaged statistical-dynamical model. Part III. The parameterization of the eddy fluxes of heat and moisture, *J. of Climate*, **3(7)**:726-740.
- VEMAP Members, 1995, Vegetation/ecosystem modeling and analysis project (VEMAP): Comparing biogeography and biogeochemistry models in a continental-scale study of terrestrial ecosystem responses to climate change and CO₂ doubling, *Global Biogeochemical Cycles* (in review).
- Vorosmarty, C.J., B. Moore III, A.L. Grace, M.P. Gildea, J.M. Melillo, B.J. Peterson, E.B. Rastetter and P.A. Steudler, 1989, Continental scale models of water balance and fluvial transport: An application to South America, *Global Biogeochemical Cycles*, **3(3)**:241-265.
- Wetherald, R.T. and S. Manabe, 1988, Cloud feedback processes in a general circulation model, *J. of Atmospheric Sciences*, **45**:1397-1415.
- Whittaker, R.H. and G.E. Likens, 1973, Primary production: The biosphere and man, *Human Ecology*, **1**:357-369.
- Willmott, C.J., M.R. Clinton and W.D. Philpot, 1985, Small-scale climate maps: A sensitivity analysis of some common assumptions associated with grid-point interpolation and contouring, *American Cartographer*, **12(1)**:5-16.
- Wilson, C.A. and J.F.B. Mitchell, 1987, A doubled CO₂ climate sensitivity experiment with a global climate model including a simple ocean, *J. of Geophysical Research*, **92**:13,315-13,343.
- Woodward, F.I. and I.F. KcKee, 1991, Vegetation and climate, *Environment International*, **17**:535-546.
- Yao, M.S. and P.H. Stone, 1987, Development of a two-dimensional zonally averaged statistical-dynamical model. Part I: The parameterization of moist convection and its role in the general circulation, *J. of Atmospheric Sciences*, **44(1)**:65-82.
- Zhang, X., 1993, A vegetation-climate classification system for global change studies in China, *Quaternary Sciences*, **2**:157-169 (in Chinese with English abstract).

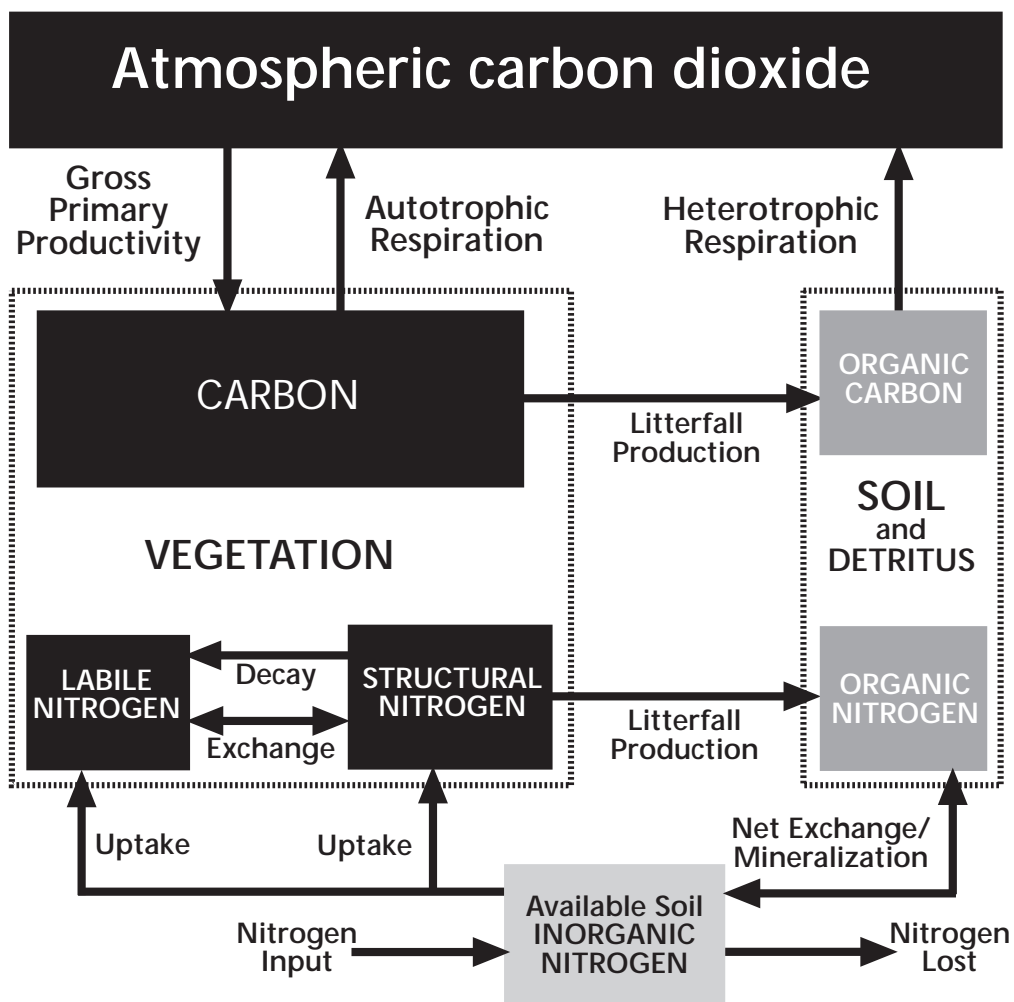


Figure 1. The Terrestrial Ecosystem Model (TEM). The state variables are: carbon, structural nitrogen, and labile nitrogen in vegetation; organic carbon and organic nitrogen in soils and detritus; and available soil inorganic nitrogen. Arrows show carbon and nitrogen fluxes: gross primary productivity; autotrophic and heterotrophic respiration; litterfall production; uptake into, and exchange between, the structural and labile nitrogen pools of the vegetation; resorption from decaying tissue into the labile nitrogen pool of the vegetation; net mineralization of soil organic nitrogen; nitrogen inputs from outside of the ecosystem; and nitrogen loss from the ecosystem. (From Melillo et al., 1993.)

Figure 2. The zonal mean changes of annual mean temperature, annual precipitation and annual mean cloudiness between $1 \times \text{CO}_2$ and $2 \times \text{CO}_2$ simulations by the 2-D MIT L-O climate model and the 3-D GISS and GFDL-q GCMs along the latitudinal bands. (The latitudinal bands are from the 2-D MIT L-O climate model.)

Figure 3. Latitudinal distributions of annual net primary production (NPP), reactive soil organic carbon (SOC), and total carbon storage (TOC) for the contemporary climate with 315 ppmv CO_2 , and land area along the 0.5° resolution latitudinal bands. Vegetation carbon is the difference between total carbon storage and reactive soil organic carbon.

Figure 4. Latitudinal distributions of the projected changes in annual net primary production (NPP) and total carbon storage for the 2-D MIT L-O climate and the 3-D GISS and GFDL-q climate with 522 ppmv CO_2 along the 0.5° resolution latitudinal bands.